sustainability

MDPI

Article

Activated Carbon and P-Rich Fertilizer Production from Industrial Sludge by Application of an Integrated Thermo-Chemical Treatment

Andrea Salimbeni [1,2,*], Marta Di Bianca [1,3], Andrea Maria Rizzo [1,2,*] and David Chiaramonti [1,4]

[1] Renewable Energy Consortium for Research and Demonstration (RE-CORD), Viale Kennedy, 182, 50038 Scarperia e San Piero, Italy; marta.dibianca@re-cord.org (M.D.B.); david.chiaramonti@polito.it (D.C.)
[2] Department of Industrial Engineering, University of Florence, Via di S. Marta, 3, 50139 Florence, Italy
[3] Department of Civil and Environmental Engineering, University of Florence, Via di S. Marta, 3, 50139 Florence, Italy
[4] "Galileo Ferraris" Energy Department, Polytechnic of Turin, Corso Duca degli Abruzzi, 24, 10129 Turin, Italy
* Correspondence: andrea.salimbeni@re-cord.org (A.S.); andreamaria.rizzo@re-cord.org (A.M.R.)

Abstract: The cost and environmental impact of sludge disposal methods highlight the necessity of new solutions for resource recovery. This study aims at concurrently producing activated carbon while recovering phosphorous by applying an integrated thermo-chemical treatment to a sludge of industrial origin. The sludge was first subjected to slow pyrolysis on a laboratory scale at different temperatures, and the produced chars were processed by leaching to obtain biocoal. Leaching tests enabled us to define the optimal slow pyrolysis temperatures to maximize leaching performances. Then, sludge was processed in a slow pyrolysis pilot-scale plant, and the produced char was subjected to acid leaching and finally to physical activation. Chemical precipitation was then applied to the liquid leachate to recover phosphorous as a salt. Laboratory-scale slow pyrolysis and leaching tests showed that a higher pyrolysis temperature leads to a lower degree of demineralization by leaching. Leaching enabled us to reduce the char ash content by almost 88%, extracting 100% P, Mg, Ca, and Fe and almost 90% Al. Physical activation of biocoal with CO_2 at 700 and 800 °C produced materials with a surface area of 353 and 417 m^2 g^{-1}, respectively, that make them potentially applicable as adsorbents in wastewater treatment or in industrial emissions processes. Moreover, the activated carbons showed the atomic H/C and O/C ratios of anthracite, which opens a wide range of alternative market applications to fossil coal, such as metallurgy and the advanced material sector. In addition, the high P and K concentrations in the salt obtained by precipitation make it a promising fertilizing product in line with the current regulations.

Keywords: phosphorus; biocoal; pyrolysis; chemical leaching; raw materials; activated carbon

Citation: Salimbeni, A.; Di Bianca, M.; Rizzo, A.M.; Chiaramonti, D. Activated Carbon and P-Rich Fertilizer Production from Industrial Sludge by Application of an Integrated Thermo-Chemical Treatment. *Sustainability* **2023**, *15*, 14620. https://doi.org/10.3390/su151914620

Academic Editors: Édgar Ricardo Oviedo-Ocaña and Viviana Sanchez-Torres

Received: 29 August 2023
Revised: 27 September 2023
Accepted: 7 October 2023
Published: 9 October 2023

1. Introduction

Europe's water is becoming a critical resource to be preserved. Economic activities, urbanization, and global warming affect the quality and availability of European freshwaters. For that, the collection and treatment of waste waters is one key element in the development of a sustainable water cycle [1]. In the European Union (EU) context, industry is considered a key stakeholder in water consumption, from both a quantitative and qualitative point of view. The uptake of water by industry in Europe represents about 54% of the total uptake for human activities, equal to about 96 billion cubic meters per year [2].

According to the Urban Waste Water Treatment Directive, the wastewater treatment processes in the EU have strongly improved from 1990 to 2014 [3]. and the number of wastewater treatment plants (WWTPs) has increased. Nowadays, 26523 urban wastewater treatment plants are operating in the EU [4]. In addition, at least 30,000 large industrial facilities with related wastewater treatment systems should be considered [5].

The growing number of wastewater treatment plants in the EU brings about a rapid increase in the amount of sludge being produced. In this respect, the annual production of dry sewage sludge in the 32 member countries of the European Environment Agency (EEA) was estimated at around 11.1 million t in 2018 [6]. Of the total sludge produced, 34% was used in agriculture, 31% was incinerated, 12% was used in compost and other applications, 12% was disposed of in landfills, and 10% was used in different ways [7].

The costs attributed to sludge management range from 20% to 65% of the overall expenses of a wastewater treatment plant [8], and they are mainly related to the high disposal cost, which currently ranges between EUR 160 and 310 t^{-1} [9]. In fact, sludge contains, on a dry basis, 50–70% organic matter, 30–50% inorganics, 3.4–4.0% N, 0.5–2.5% P, 1–3% Al, and micronutrients [10,11], but also sulfur, heavy metals, and organic compounds that are toxic for the environment, such as polycyclic aromatic hydrocarbons (PAHs), surfactants, pharmaceuticals, and others [12].

Another relevant cost item for WWTPs is energy consumption, which contributes to WWTP operational costs by about 7–33% [13]. For this reason, to improve the economics and sustainability of both industrial and municipal WWTPs, sludge management should be based on the effective recovery of nutrients and carbon while minimizing energy consumption. The recovery of phosphorus from sludge is particularly supported by several EU member states. Phosphate rock extraction increased from 3.4 million metric t in 1913 to 245 million metric t in 2014 [14], with a projection of 425 million metric t by 2050 [15], so that the EU has identified phosphate rock and phosphorous among the 34 critical raw materials of high importance for the EU economy and of high risk associated with their supply [16].

However, Regulation (EU) 2019/1009 on fertilizing products (EU FPR) [17] excludes both municipal and industrial sludge from being used for CE organic fertilizer production. Despite the fact that sludge is still used in agriculture, or at small percentages, for compost production in many EU countries, EU FPR prevents compost, digestate, or biochar from sludge from being certified as CE fertilizing products. On the contrary, inorganic fertilizers and precipitated phosphate salts, extracted from wastewater, are strongly promoted [14–16,18,19].

Organic carbon is the other key element of sludge. In fact, organic carbon does not only represent the main element contained in sludge, but it is also a high-value product today. In fact, the carbon value is strictly related to that of CO_2. By the European Union European Trading Scheme (EU ETS) regulation, which establishes the market mechanism attributing CO_2 a price [20], any ton of CO_2 emitted by the steel, energy, or fertilizer sector corresponds to an allowance that the company in that sector must purchase. The stricter measures adopted by the recently updated version of the EU ETS made CO_2 prices reach prices between EUR 80 and 100 t^{-1} [21]. Since the EU ETS will include municipal waste incineration plants as of 2026, any ton of carbon in the sludge, if incinerated, will represent a high cost for the incineration plant (around EUR 240 t^{-1}, at the current CO_2 price of EUR 80 t^{-1}). An alternative use, preferably a carbon storage solution, could reduce fossil coal consumption and avoid CO_2 emissions. In the context of reducing sludge volumes and maximizing the recovery of sludge, water removal represents the first challenge. To this end, innovative sludge dewatering and pre-treatment technologies, such as vacuum preloading, freeze-thaw, and Fenton treatment, have been recently investigated, with promising results in terms of water removal and low energy consumption [22,23]. The results achieved by advanced dewatering systems must be considered as the starting point for a sustainable valuation of sludge as a source of valuable materials.

Thermochemical treatments of sludge, such as hydrothermal carbonization (HTC), slow pyrolysis, and hydrothermal liquefaction (HTL), have been the subject of several studies as an alternative to its incineration [24,25].

Among them, the HTC and slow pyrolysis processes are known as “carbonization processes”, due to their main aim of maximizing carbon recovery as a solid material.

The HTC process works at temperatures in the range of 180–250 °C and pressures in the range of 10–50 bar and operates in a reaction environment characterized by the presence of liquid water [13]. The two main products of HTC are the solid, named "hydrochar", which is a carbonaceous, highly volatile solid, namely >50% dry basis (d.b.), and the water phase, rich in organic carbon [26]. For this reason, HTC is also seen as a pre-treatment preceding the application of other recovery processes, such as anaerobic digestion of the water phase and pyrolysis of the hydrochar [27,28].

Slow pyrolysis needs sludge to be previously dewatered by drying or other pre-treatment systems. The process works at higher temperatures, in a range between 400 and 700 °C, with a residence time in the order of hours and heating rates between 1 and 20 °C/min [29,30]. The process always generates three products: a solid carbonaceous matrix (char), a mixture of condensable vapors (water and organic compounds), and a mixture of permanent gases (CO, CO_2, CH_4, H_2, etc.) [31]. After pyrolysis, most of the sludge's ashes are concentrated in the char, which usually represents more than 40% d.b. of the processed material, rising to over 50% d.b. in the case of ash-rich municipal sludges [32]. Consequently, an effect of treating sludge by slow pyrolysis is the increase of the ash content in the produced char and often, by consequence, a reduction of the carbon content in comparison with the processed feedstock.

Char is a carbonaceous product, rich in inorganics when produced by sludge, hydrophobic, and with a low volatile content. Phosphorous, as well as calcium, iron, and silicon, are more concentrated in char compared to the processed feedstock. Due to its high ash content and its low heating value (9–14 MJ kg^{-1} d.b.), char from sludge slow pyrolysis is neither suitable as a solid biofuel nor applicable in the steel industry. However, the high concentration of both inorganic compounds and carbon makes sludge-derived char an interesting raw material that is usable as a source of nutrients and renewable carbon.

The scientific challenge of sludge management consists then in the valuation of resources from this waste, including carbon and inorganic compounds (with phosphorous in the first place). To this end, a chemical char upgrading step to extract phosphorus and other inorganic compounds could represent not only a promising solution to ensure a full valorization of these raw materials but also an opportunity to improve char quality and unlock its potential application in the cement, steel, and other industry sectors.

Chemical leaching is a process that allows for the separation of the soluble components of a solid material by dissolving them into a liquid phase. A common application of chemical leaching is low-grade coal cleaning, aiming to reduce the amount of mineral matter [15], which comprises ash and sulfur [16]. The application of the acid leaching process for phosphorus extraction from pyrolyzed sludge has been tested by the authors in previous studies with promising results. Acid leaching performed on sludge-derived char enabled a high extraction rate of P, Ca (>90%), and other metals; at the same time, the process extracted only 50% of Al and was ineffective on SiO_2 extraction [32]. The products obtained by the acid leaching process applied to sludge-derived char consist of an acid liquid containing the recovered inorganic elements, such as P, Ca, and Fe, and a biocoal (LBC), with a higher C content compared to the raw char and a reduced ash concentration. The inorganic elements retained in the liquid can be recovered by chemical precipitation, producing an inorganic compound with a high N, P, and K content. Biocoal, with its reduced ash content and, thus, increased carbon content, can be considered an alternative as a precursor for the production of adsorbents and biomaterials.

To the best of the authors' knowledge, many studies are available concerning the extraction of phosphorus from sludge ash [33–35] or the production of biochar by slow pyrolysis [36,37]. However, limited literature was found addressing the simultaneous valorization of both carbon and phosphorus retained in sewage sludge, mainly involving hydrothermal carbonization as a thermochemical treatment process [38,39], characterized by high volatility and low market value. The aim of the proposed work is to test the integrated slow pyrolysis and acid leaching processes on an ash-rich industrial sludge to obtain a low-ash biocoal and extract most of the valuable inorganic elements. This integrated

process was previously tested by the authors on an ash-rich municipal sewage sludge [25], but never before on a sludge of industrial origin. Moreover, this study investigated the extraction of inorganics from the leachate by chemical precipitation and the upgrading of the biocoal by means of physical activation to produce two high-value products: an inorganic N-P-K fertilizer in compliance with the EU FPR regulation and an activated carbon with high micro- and meso-porosity, reusable for wastewater treatment or as an alternative to fossil coal in different sectors.

2. Materials and Methods

2.1. Feedstock: Industrial Sludge

The feedstock consists of an industrial sludge generated by anaerobic digestion, centrifuging, and drying of the suspended solids from the WWTP of an Italian meat producer factory. The WWTP producing the sludge receives the waste streams of the agri-food production, the meat manufacturing process, and the wastewater of the whole industrial complex, including equipment washing, toilets, and other facilities.

2.2. Experimental Activity

2.2.1. General Description of the Experimental Activity

The experimental campaign started with slow pyrolysis testing at laboratory scale, performed at different operating temperatures. Then, the leaching of the produced chars was tested, aiming to assess the performance of the leaching process on char produced at different pyrolysis temperatures. Based on the results of the leaching and pyrolysis tests, the most promising operating conditions for the slow pyrolysis test were selected. In particular, the temperature and the residence time chosen for the pilot-scale pyrolysis tests are those that enabled the highest degree of demineralization in the laboratory. Subsequently, the char from the slow pyrolysis pilot scale test was leached, adopting more severe conditions compared to those tested in the laboratory in order to maximize the ash extraction efficiency. The dissolved inorganic compounds were recovered from the leachate by precipitation. Finally, the activation process for the biocoal was tested. The activities performed during the experimental campaign are described in the paragraphs below.

2.2.2. Laboratory-Scale Slow Pyrolysis Tests

Sludge slow pyrolysis tests in laboratory (PT_{400}–PT_{650}) were performed on a thermogravimetric analyzer (LECO TGA701). Six pyrolysis tests were carried out at constant residence time (1 h) and heating rate (20 °C min^{-1}), increasing the temperature by 50 °C, from 400 °C to 650 °C, among the tests. The following nomenclature is adopted to identify the laboratory-scale slow pyrolysis tests:

- PT_{400}: test performed at the pyrolysis temperature of 400 °C;
- PT_{450}: test performed at the pyrolysis temperature of 450 °C;
- PT_{500}: test performed at the pyrolysis temperature of 500 °C;
- PT_{550}: test performed at the pyrolysis temperature of 550 °C;
- PT_{600}: test performed at the pyrolysis temperature of 600 °C;
- PT_{650}: test performed at the pyrolysis temperature of 650 °C.

The mass yield was determined for each trial, and the char from each test was then analyzed in laboratory. The carbon recovery rate was calculated for each test, after char characterization, as follows:

$$C\ recovery\ rate\ (\%) = \frac{C\ BC \cdot mass\ BC}{C\ sludge \cdot mass\ sludge} \quad (1)$$

where *C BC* (% d.b.) and *mass BC* (g) are the carbon content and the mass of the char (BC) from the test, respectively, and *C sludge* (% d.b.) and *mass sludge* (g) are the carbon content and the mass of the processed dry industrial sludge, respectively.

2.2.3. Pilot-Scale Slow Pyrolysis Test

A pilot-scale slow pyrolysis unit (Figure 1) was operated for the test in a real-world environment. The pyrolysis unit, called SPYRO, is an auger-type reactor of approximately 2 m in length and an inner diameter of 0.15 m. The unit can convert up to 3 kg h^{-1} of feedstock and can be operated up to 600 °C. The pyrolysis reactor is coupled with a condensation unit for the recovery of volatiles in the form of pyrolysis liquid. Details of the pilot unit are reported elsewhere [32].

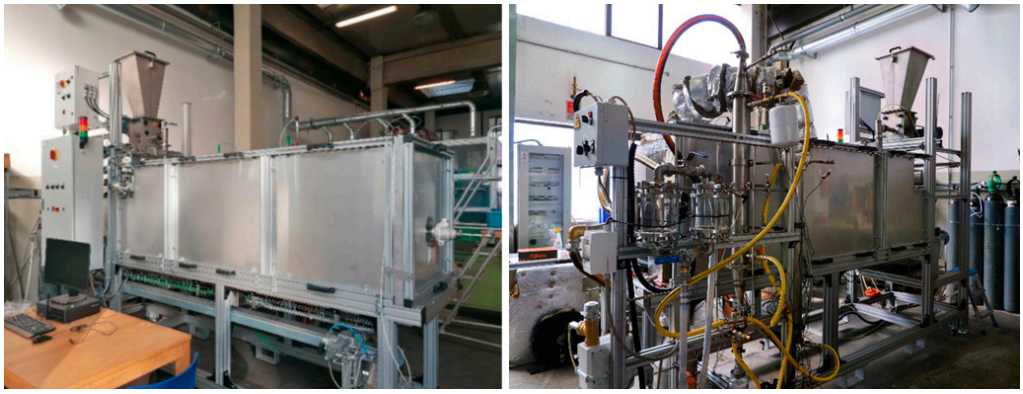

Figure 1. Slow pyrolysis pilot unit (RE-CORD experimental area).

The operational parameters of the pilot-scale slow pyrolysis test (PT_P) are shown in Table 1. The rotating speed of the reactor screw was set at 0.4 rpm to achieve a solid residence time of almost 1 h.

Table 1. Operational parameters of the pilot-scale slow pyrolysis test (PT_P).

Operational Parameter	PT_P	Unit
Feeder frequency	8	Hz
Auger screw rotational speed	0.3	rpm
Solid residence time	60	min
Heating rate	20	°C min^{-1}
Set temperatures	400/400/450	°C

The char produced by the trial was collected and weighted to calculate char mass yield (*PMY*) as follows:

$$PMY = \frac{BC_P\ mass}{sludge\ mass} \cdot 100 \quad (2)$$

where BC_P *mass* (g) is the mass of char and *sludge mass* (g) is the mass of dry sludge.

Then the char was analyzed. The pyrolysis oil obtained by the pilot plant condensation system was first collected and weighted, and then separated gravimetrically, obtaining three phases: a light oil phase (LOP), an aqueous phase (AP), and a heavy oil phase (HOP). After collection, the LOP and the HOP were analyzed.

2.2.4. Experimental Procedures for Chemical Leaching Tests

The char samples obtained from slow pyrolysis tests on the lab scale (BC) and on the pilot scale (BC_P) were processed by chemical leaching. The experimental campaign was conducted at laboratory scale to extract and separate the desired inorganic elements from the char. First, chemical leaching tests were performed to identify the optimal leaching operating conditions. The following operating conditions were varied during the experiments:

- Mass ratio between leaching solution and processed char (liquid:char);
- Pure reagent concentration (HNO_3) in the leaching solution (molarity, mol L^{-1});

- Operating temperature (temperature, °C);
- Contact time (contact time, h).

All the leaching tests were performed using the same procedure. Char was initially oven dried at 105 °C to a constant weight. The leaching solution was prepared by mixing, in a beaker, demineralized water and nitric acid (dosed as a ≥65% solution by Honeywell, ACS grade). The char was ground manually at a size below 500 µm in the case of BC processing and below 250 µm in the case of BC_P, and then added to the solution. Each test was performed using a heating plate equipped with a thermocouple and a magnetic stirrer. At the end of the contact time, the contents of the beaker were vacuum filtered to separate the liquid from the solid phase. The separated solid material was then washed with demineralized water for 30 min to remove the residual acid reagent. The separation of washing water was again performed through vacuum filtration. The solid material was finally oven-dried at 105 °C to a constant weight.

2.2.5. Performance Indicators of Chemical Leaching Tests

Leaching test performances were evaluated by two indicators: degree of demineralization (*DD*) and element extraction efficiency (*EE*).

The first, calculated for all leaching tests, expresses the percentage of extracted ash against the initial content in the processed char:

$$DD\ (\%) = \frac{ash\ BC - ash\ LBC}{ash\ BC} \quad (3)$$

where *ash BC* (% d.b.) is the ash in the processed char, and *ash LBC* (% d.b.) is the ash in the biocoal.

The second indicator was calculated for the leaching test performed on BC_P (LT_P) only and expresses the percentage of the extracted element against the initial content of that element in the processed char:

$$EE\ (\%) = \frac{element\ LL}{element\ BC,i} \cdot 100 \quad (4)$$

where *element LL* (mg) is the element mass in the leachate (LL), and *element BC,i* (mg) is the element mass in the processed char. Both were calculated given the mass of the LL and processed char, and the element concentration in the materials was determined analytically.

2.2.6. Chemical Leaching Tests on BC from Laboratory-Scale Slow Pyrolysis Tests

To select the process conditions to be performed in the slow pyrolysis pilot plant, the study included an assessment of the impact of slow pyrolysis temperatures on the efficacy of the leaching process in terms of inorganic compound extraction. Six chemical leaching tests at the same conditions were performed, processing the chars (BC) produced in the laboratory at different temperatures. In each test, 11.2 g of char were processed. The tests were performed using nitric acid (HNO_3) as a reagent and under the following operating conditions: liquid:char 10:1, molarity 0.5 mol L^{-1}, temperature 30 °C, and contact time 1 h. The following nomenclature is adopted to identify the chemical leaching tests:

- LT_{400}: test performed on the BC from PT_{400};
- LT_{450}: test performed on the BC from PT_{450};
- LT_{500}: test performed on the BC from PT_{500};
- LT_{550}: test performed on the BC from PT_{550};
- LT_{600}: test performed on the BC from PT_{600};
- LT_{650}: test performed on the BC from PT_{650}.

The samples of biocoal (LBCs) were collected, and their ash content was determined.

2.2.7. Chemical Leaching Tests on BC from PT_P

Finally, a chemical leaching test was performed on the char produced by the pilot-scale pyrolysis test (BC_P), aiming to extract the inorganics from the char and maximize the ash reduction in the final solid. In this test, 20 g of char in a 0.8 M HNO_3 acid solution were processed with a contact time of 2 h and a temperature set at 70 °C. The solid mass yield was calculated for the leaching test performed on BC_P (LT_P), assuming that no organic matter is lost during the leaching process (neither in liquid nor in gas form). The equation adopted is the following:

$$LMY = \frac{((ash\ LBC \cdot (mass\ BC - mass\ BC \cdot ash\ BC)\ /\ (1 - ash\ LBC)\ ) + (mass\ BC - mass\ BC \cdot ash\ BC))}{mass\ BC_P} \quad (5)$$

where:

- *LMY*—Leaching Mass Yield (% d.b.);
- *Ash LBC*—Ash content of biocoal (% d.b.);
- *Mass* BC_P—Mass of processed char (g);
- *Ash* BC_P—Ash content of processed char (% d.b.).

The outcome of the laboratory trials was used to define the process conditions for the pilot-scale slow pyrolysis test and for the chemical leaching test on the processed char.

2.2.8. Chemical Precipitation Test

The leachate from the LT_P was adopted as the starting material for the precipitation test, aiming at recovering the inorganic compounds dissolved in the liquid in solid form by increasing the liquid pH. To this end, known volumes of a KOH solution were dosed in the glass beaker containing the acid liquid. During the process, the system was stirred, and the pH was monitored by a pH meter (Metrohm 827 pH). The 15% KOH solution adopted for the test was prepared by KOH pellets (≥97% purity, ACS grade by Merck). The dosage was stopped when a pH of around 9 was achieved in the liquid phase. The precipitated solid was then separated from the liquid phase by centrifugation and finally dried in an oven at 105 °C.

2.2.9. Activation Tests

The LBC from the LT_P was then activated. The activation tests (AT) were performed using a batch tubular quartz reactor placed in a ceramic furnace. The furnace is equipped with k-type thermocouples both inside and outside the reactor, controlled by a programmable logic controller (PLC). First, a known quantity of LBC_P was charged in the tubular reactor, which was then placed in the furnace. Subsequently, the desired process temperature and the heating rate were set. As a first step, nitrogen was fluxed to avoid oxygen entering and feedstock oxidation. Afterwards, CO_2 was fluxed at a flow rate of 3.5 l min^{-1} for the set residence time. During the first activation test (AT1), 9 g of LBC_P were processed, while 8 g of LBC_P were processed during AT2. The activation test operating conditions are reported in Table 2.

Table 2. Activation tests performed on the biocoal (LBC_P).

Operating Parameters	AT1	AT2	Unit
Starting material	LBC_P	LBC_P	-
Temperature	700	800	°C
Residence Time	1	1	h
Heating rate in N_2	20	20	°C min^{-1}

The activated carbon (AC) mass yield obtained by the activation test (*AMY*) was calculated for both trials as follows:

$$AMY = \frac{AC\ mass}{LBC_P\ mass} \cdot 100 \quad (6)$$

where *AC mass* (g) is the mass of activated carbon and LBC_P *mass* (g) is the mass of biocoal.

The total AC mass yield (ACY_{tot}) obtained by slow pyrolysis (PT_P), acid leaching (LTP), and activation (AT1, AT2) is calculated by the following formula:

$$ACY_{tot} = AMY \cdot LMY \cdot PMY \quad (7)$$

2.3. Feedstock and Process Product Characterization

The characterization of the sludge used as pyrolysis feedstock and of the products obtained from the tested processes consisted of different physical-chemical analyses.

The industrial sludge was first air dried to determine its moisture content prior to its characterization. The first analysis consisted of the determination of the content of residual moisture, ash, determined at 550 °C (ash 550) and 710 °C (ash 710), volatiles, and fixed carbon (fixed C, calculated as the difference between 100 and the sum of moisture, volatiles, and ash 550, according to UNI EN 1860-2: 2005), in the sludge (proximate analysis). Then, sludge C, H, N, and S content (ultimate analysis) were determined. In addition, the higher heating value (HHV) was analyzed, calculating the lower heating value (LHV) by means of the HHV, H, and moisture content (following UNI EN ISO 18125: 2018 and UNI EN ISO 16948: 2015). Finally, the concentration of metals P and Si was determined by microwave plasma atomic emission spectroscopy (MP-AES).

Char from slow pyrolysis in the pilot unit was characterized by the same analysis and instruments as the feedstock, while for the chars from laboratory-scale pyrolysis, ash 550 and 710, volatiles, and C, H, N, and S content were determined. The biocoal was characterized by its ash (550 and 710), volatiles (C, H, and N), and its composition in metals (P and Si). Activated carbons were characterized by their ash 550 and 710, C, H, and N contents, surface area, and pore volume. In addition, Fourier-transform infrared spectroscopy (FT-IR) analysis of the activated carbons was performed. The surface area of the pilot unit char, of the biocoal, and of the activated carbons was determined via the Brunauer-Emmett-Teller (BET) method, while the plots of the pore volume and of the surface area of the activated carbons were determined by the density functional theory (DFT) method. The micropore volume of the activated carbons was also derived by the alpha-S method.

The HOP and the LOP of the condensed pyrolysis oil were analyzed, determining their water content, C, H, and N content, HHV, and LHV.

The characterization of the leachate and of the precipitated compound consisted of the analysis of metal, P, and Si concentrations. The precipitated compound composition was also expressed as oxides, starting from the analytical elemental composition and considering the different molar masses.

Moisture was determined by drying the feedstock sample at 105 °C until a constant weight was reached, according to UNI EN ISO 18134-2: 2017. Ash and volatiles were determined by a thermogravimetric analyzer (LECO TGA701), following UNI EN ISO 18122: 2016 and UNI EN 1860-2: 2005 (for ash 550 and ash 710, respectively, by heating around 1 g sample up to 550 °C or 710 °C under constant air flow until constant weight was reached) and UNI EN ISO 18123: 2016 (for volatiles, by heating around 1 g sample under nitrogen flow up to 900 °C).

C, H, N, and S were determined by a CHN-S analyzer (LECO TruSpec CHN-S). C, H, and N analysis was performed according to ASTM D5291-10 for liquid samples (HOP and LOP) and to UNI EN ISO 16948: 2015 for solid materials. ASTM D 4239 was followed for S content determination. For C, H, N, and S analysis, about 60–80 mg of sample material were combusted at high temperatures (950 °C for C, H, and N and 1350 °C for S) and converted

by catalysts to carbon dioxide, water vapor, elemental nitrogen, and sulfur dioxide. Lower S content values (<0.1% *w*/*w*) were instead determined by an ion chromatography system (Metrohm 883 Basic IC Plus) after combustion by a bomb calorimeter (LECO AC500). A higher heating value (HHV) was obtained by a bomb calorimeter (LECO AC500), according to UNI EN ISO 18125:2018 for solid materials and DIN 51900-1:2000 and DIN 51900-3:2005 for liquid samples (HOP and LOP). The sample (around 0.30–1.0 g) was weighted and placed in the combustion bomb, then flushed with oxygen reaching 30 bar. Before ignition, the temperature was stabilized for 3 min; then the ignition was started by an electrical ignition device, and the temperature was monitored for 5 min. HOP and LOP water content determination was performed by Karl Fischer titration (Metrohm 848 Titrino Plus, Herisau, Switzerland), following ASTM E203-08, titrating about 0.1–0.5 g with iodine-based Karl Fischer reagents. The concentration of metals, P, and Si (inorganic elements) was determined using microwave plasma atomic emission spectroscopy (MP-AES, by Agilent 4200 MP-AES), which uses nitrogen plasma, in compliance with UNI EN ISO 16967: 2015 and UNI EN ISO 16968: 2015. For liquid samples, around 500 mg were analyzed. For the determination of inorganic elements in the organic solids (sludge, chars, and biocoal), the samples (around 30 mg each) have been previously digested with 3 mL of hydrogen peroxide and 5 mL of nitric acid in a Milestone Start D microwave digestion system to be completely solubilized in a liquid sample, then analyzed by MP-AES. Pore volume and surface area were analyzed via a surface area and pore size analyzer (Quantachrome NOVA 2200E), following ASTM D6556-10. This instrument analyzes the pore size of the samples in the range of 2–52 nm.

Before the analysis, samples were dried at 200 °C for 48 h in oven. Then they were degassed in the analyzer at 200 °C for 24 h under vacuum to remove moisture and volatile compounds. Degassed samples were then weighed in a bulb cell and analyzed after immersion in liquid nitrogen to determine the correspondent adsorption isotherm, and then the sample surface area (by BET and DFT methods) and the pore volume (by DFT method) were derived. The cumulated surface area, cumulated pore volume, and alpha-S plot of the activated carbons were generated by the software NovaWin^{TM} by Quantachrome (version 11.02).

FT-IR analysis was performed through a FT-IR Shimadzu IR Tracer 100 in attenuated total reflectance (ATR) mode with an optical resolution of 4 cm^{-1} and a spectral range from 600 to 4000 cm^{-1} averaged on 45 scans.

3. Results

3.1. Feedstock Characterization

The characterization of the processed industrial sludge is reported in Tables 3 and 4.

Table 3. Proximate analysis and ultimate analysis of the processed industrial sludge.

Element	Value	Unit
Moisture	33.8	% w.b.
Ashes (550 °C)	26.0	% d.b.
Ashes (710 °C)	26.0	% d.b.
Volatiles	66.7	% d.b.
Fixed C	7.3	% d.b.
Carbon (C)	39.5	% d.b.
Hydrogen (H)	5.7	% d.b.
Nitrogen (N)	7.0	% d.b.
Sulfur (S)	2.3	% d.b.
Higher heating value (HHV)	18.1	MJ/kg d.b.
Lower heating value (LHV)	16.9	MJ/kg d.b.

w.b.—wet basis. d.b.—dry basis.

Table 4. Inorganic elements concentration in the processed industrial sludge.

Element	Value	Unit
Al	4730	mg/kg d.b.
Ca	42,802	mg/kg d.b.
Cr	46	mg/kg d.b.
Cu	67	mg/kg d.b.
Fe	51,777	mg/kg d.b.
K	2034	mg/kg d.b.
Mg	2324	mg/kg d.b.
Mn	455	mg/kg d.b.
Na	1638	mg/kg d.b.
Ni	b.d.l.	mg/kg d.b.
P	20,043	mg/kg d.b.
Pb	16	mg/kg d.b.
Si	1576	mg/kg d.b.
Ti	26	mg/kg d.b.
Zn	416	mg/kg d.b.

d.b.—dry basis.

3.2. Laboratory-Scale Slow Pyrolysis Tests

The char mass yield, the ash content, the volatiles content, and the C, H, N, and S content of the char obtained by the six laboratory-scale slow pyrolysis tests are reported in Table 5.

Table 5. Mass yield and composition of the chars from the laboratory scale slow pyrolysis trials (PT_{400}–PT_{650}: slow pyrolysis test at 400–650 °C).

Parameter	PT_{400}	PT_{450}	PT_{500}	PT_{550}	PT_{600}	PT_{650}	Unit
Char mass yield	52.4	46.8	44.3	42.7	41.7	38.0	% d.b.
Ashes (710 °C)	54.1	59.5	61.6	65.5	66.9	68.7	% d.b.
Volatiles	28.0	24.4	22.4	20.2	19.0	16.7	% d.b.
Total carbon (C).	35.1	31.4	31.8	29.9	29.7	30.4	% d.b.
Total hydrogen (H)	2.4	1.5	1.2	0.9	0.8	0.6	% d.b.
Total nitrogen (N)	6.1	5.8	5.7	5.2	4.7	3.9	% d.b.
Total sulfur (S)	2.65	2.95	3.11	3.38	3.36	3.0	% d.b.
Atomic H/C	0.8	0.6	0.4	0.3	0.3	0.2	% d.b.

d.b.—dry basis.

The carbon recovery rate in the solid product is shown in Figure 2.

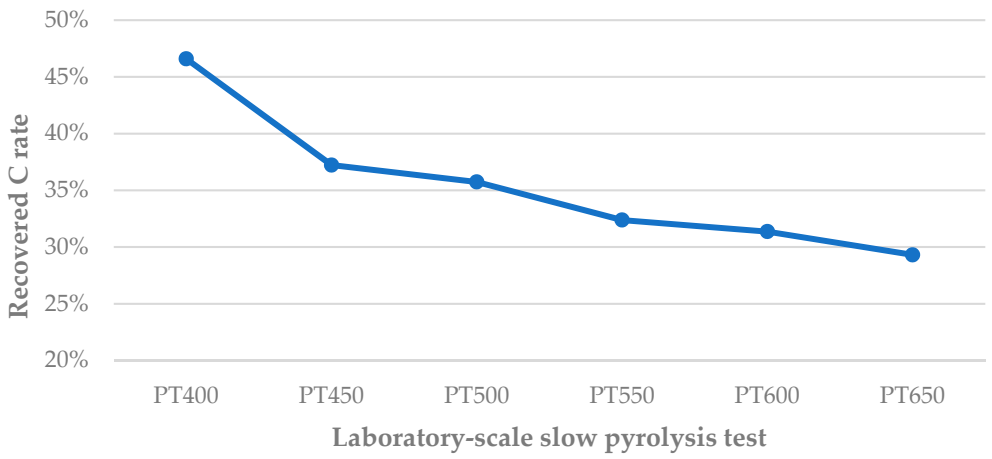

Figure 2. Recovered carbon rate (recovered C rate) in the char at different slow pyrolysis temperatures (PT400–PT650: laboratory scale slow pyrolysis test at 400–650 °C).

As reported in the graph, over 45% of carbon was recovered as solid material produced at 400 °C, around 35% at 500 °C, and less than 30% at 650 °C.

3.3. Effect of Pyrolysis Temperature on Leaching Process Performances

The efficacy of the leaching process on the char obtained at different pyrolysis temperatures (400, 450, 500, 550, 600, and 650 °C) under the same chemical leaching conditions was evaluated by calculating the DD of each test. The trend of the DD against pyrolysis temperature is reported in Figure 3.

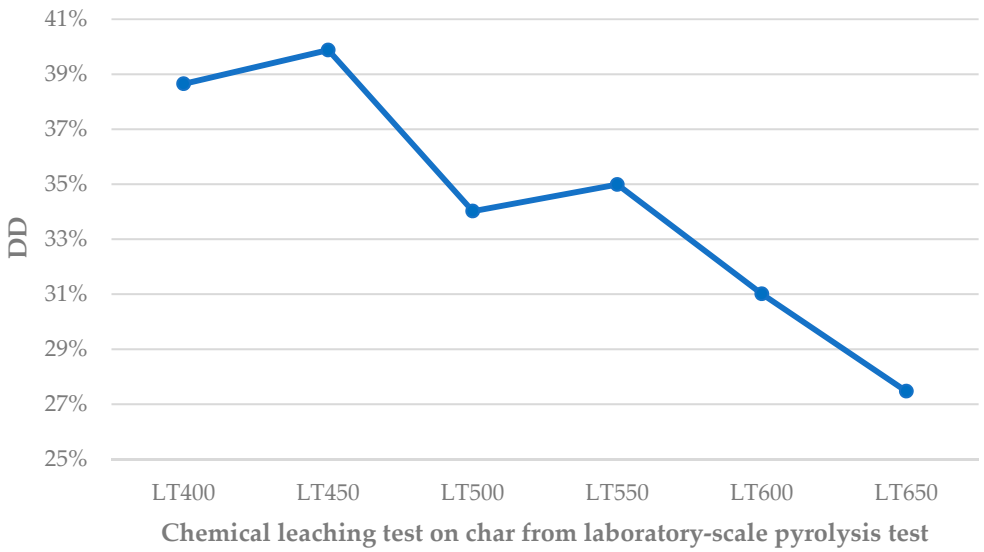

Figure 3. Degree of demineralization (DD) of the chemical leaching process on char produced at different pyrolysis temperatures (LT400–650: leaching test on char produced from a laboratory-scale slow pyrolysis test at 400–650 °C).

3.4. Pilot-Scale Slow Pyrolysis Test

3.4.1. Mass Balance

The comprehensive mass balance of the pilot-scale slow pyrolysis test is reported in Table 6. During the slow pyrolysis trial performed in the pilot plant, 3.71 kg of dry industrial sludge were processed, producing 1.60 kg of char, 1.27 kg of condensate, and about 0.84 kg of permanent gases, calculated by difference (Table 6). By gravimetric separation, the following pyrolysis oil fractions have been collected:

- Light oil phase (LOP): a brown color, homogeneous oil phase lighter than water, containing organic compounds, which represented about one-thirds of the condensed fraction;
- Aqueous phase (AP): a gray liquid containing mainly water and representing about two-thirds of the condensable fraction collected;
- Heavy oil phase (HOP): a black oil phase heavier than oil, rich in aromatic compounds, such as TAR, amounting to less than 2% of the total condensates.

The recovered products, characterized according to the methodology explained above, are described in the paragraphs below.

The mass yields of the pilot-scale test are also represented graphically in Figure 4.

The carbon balance resulting from the pyrolysis trial showed that 39% of the feedstock carbon remained in the solid, while 61% devolatilized as process gas. This result was similar to that achieved in the laboratory under the same process conditions, in which 37% carbon was recovered in the char. In addition, 38% of the feedstock nitrogen was recovered in the solid pyrolysis product (BC_P) and 33% in the two oil phases.

Table 6. Mass balance of the pilot-scale slow pyrolysis test (AP: Aqueous Phase, LOP: Light Oil Phase, HOP: Heavy Oil Phase).

Material	Mass (kg)	Mass Yield (%)
Industrial sludge (dry)	3.71	-
Char	1.60	43.1
Pyrolysis oil	1.27	34.2
of which:		
• LOP	0.40	11.3
• AP	0.85	22.3
• HOP	0.02	0.5
Permanent gases	0.84 *	22.6

* Calculated by difference.

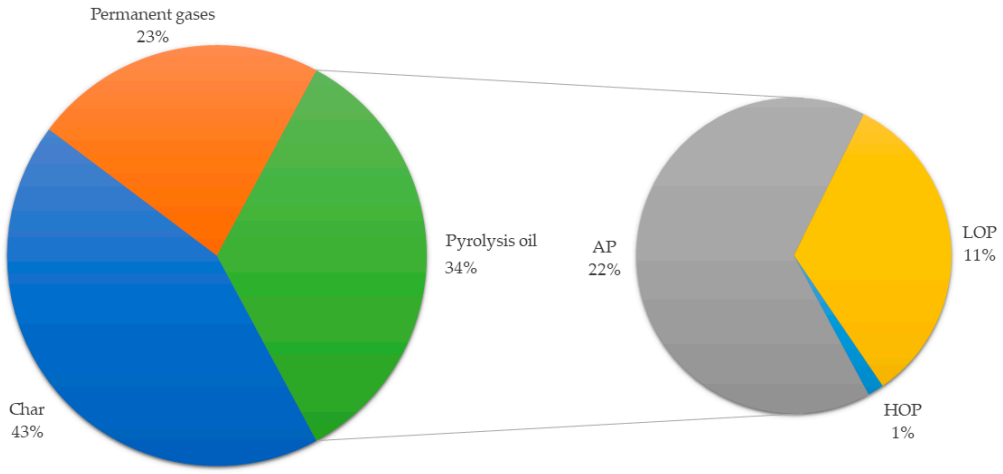

Figure 4. Pyrolysis products distribution after the pilot-scale slow pyrolysis trial (AP: Aqueous Phase, LOP: Light Oil Phase, HOP: Heavy Oil Phase).

3.4.2. Energy Balance

The theoretical chemical energy input to the pyrolysis plant in the form of dry sludge was about 62.5 MJ, calculated by multiplying the processed feedstock mass by its calorific value. The energy recovered as pyrolysis products, calculated using the same methodology, is distributed as follows: 22.4 MJ in the char, 13.4 MJ in the condensates, and 26.7 MJ in the gas (calculated as a difference). The extracted char contained about 36% of the feedstock chemical energy, while 22% was recovered in the condensed pyrolysis oil and 42% in the permanent gases, as shown in Figure 5.

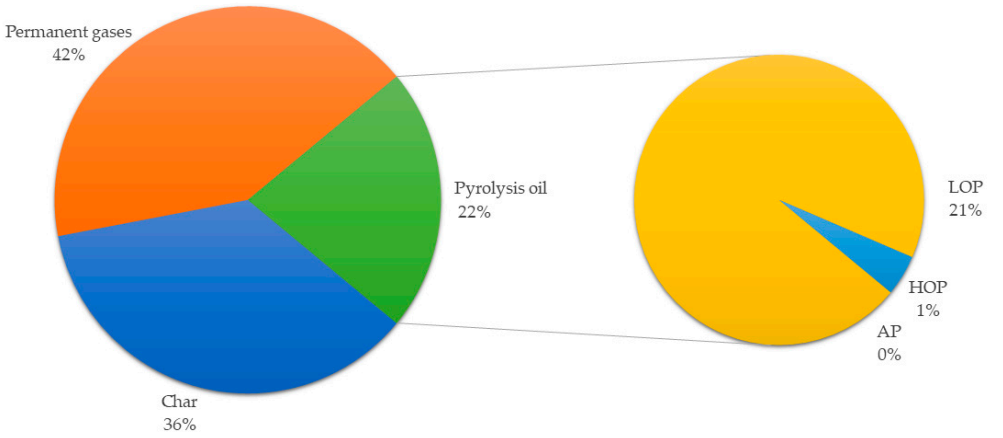

Figure 5. Chemical energy distribution among the different pyrolysis products after the pilot-scale slow pyrolysis trial (AP: Aqueous Phase, LOP: Light Oil Phase, HOP: Heavy Oil Phase).

3.4.3. Pyrolysis Oil Characterization

The results of the two oil fraction characterizations (LOP and HOP) are shown in Table 7.

Table 7. Composition of LOP (Light Oil Phase) and HOP (Heavy Oil Phase).

Material	Parameter	Value	Unit
LOP	Carbon (C)	62.5	% w.b.
	Hydrogen (H)	9.2	% w.b.
	Nitrogen (N)	7.5	% w.b.
	Higher heating value (HHV)	34.1	MJ/kg w.b.
	Lower heating value (LHV)	32.1	MJ/kg w.b.
	Water content	8.6	% w.b.
HOP	Carbon (C)	61.0	% w.b.
	Hydrogen (H)	8.1	% w.b.
	Nitrogen (N)	6.7	% w.b.
	Higher heating value (HHV)	28.7	MJ/kg w.b.
	Lower heating value (LHV)	27.0	MJ/kg w.b.
	Water content	10.5	% w.b.

w.b.—wet basis.

Both LOP and HOP showed a carbon content higher than 60% and a relevant nitrogen content of 7.5% and 6.7%, respectively. The low water content of the oil phases results in an oil of high calorific value, which could be of interest for potential energy valorization. However, the concentration of nitrogen could contribute to the formation of fuel NOx during combustion.

3.4.4. Char from Pilot-Scale Test (BC_P) Characterization

The results of BC_P characterization are reported in Tables 8 and 9.

Table 8. Proximate and ultimate analysis and surface area of BC_P (char from the slow pyrolysis test at pilot scale).

Parameter	Value	Unit
Ashes (550 °C)	56.4	% d.b.
Ashes (710 °C)	56.1	% d.b.
Volatiles	23.6	% d.b.
Fixed C	20.0	% d.b.
Total carbon (C)	35.4	% d.b.
Total Hydrogen (H)	1.8	% d.b.
Total Nitrogen (N)	6.2	% d.b.
Total Sulfur (S)	2.5	% d.b.
Higher heating value (HHV)	14.4	MJ/kg d.b.
Lower heating value (LHV)	14.0	MJ/kg d.b.
Surface area	7.6	m^2g^{-1} d.b.

d.b.—dry basis.

Table 9. Inorganic elements concentration in BC_P (char from slow pyrolysis test at pilot scale).

Element	Value	Unit
Al	10,308	mg/kg d.b.
Ca	71,974	mg/kg d.b.
Cr	108	mg/kg d.b.
Cu	169	mg/kg d.b.
Fe	93,122	mg/kg d.b.
K	4758	mg/kg d.b.
Mg	5683	mg/kg d.b.
Mn	1052	mg/kg d.b.

Table 9. *Cont.*

Element	Value	Unit
Na	3862	mg/kg d.b.
Ni	43	mg/kg d.b.
P	33,601	mg/kg d.b.
Pb	18	mg/kg d.b.
Ti	55	mg/kg d.b.
Zn	937	mg/kg d.b.

d.b.—dry basis.

BC_P shows a higher ash content compared to the starting industrial sludge due to organic matter volatilization and consequent ash concentration, as mineral matter does not take part in the pyrolysis process. Consequently, the concentration of volatiles is lower compared to the starting sludge, while the fixed carbon content is higher. The concentration of metals, phosphorous, and silicon is higher.

3.5. Chemical Leaching Test on BC_P

3.5.1. Performances of Chemical Leaching Tests on BC_P

The extraction efficiency of key inorganic elements is reported in Figure 6. The chemical leaching process applied to BC_P enabled the extraction of high percentages of P, Ca, and other inorganic elements contained in the char. A DD of 87.5% was achieved, reducing the ash content in the char from an initial value of 56.1% d.b. to a final value in the biocoal of 9.2% d.b. The high DD led to a high extraction efficiency for most of the inorganic elements. In particular, an EE of 100% was achieved for valuable elements like P, Mg, Ca, and Fe, and an extraction close to 90% for Al and K. These values are confirmed by the elemental analysis of the LBC_P reported in Section 3.5.2.

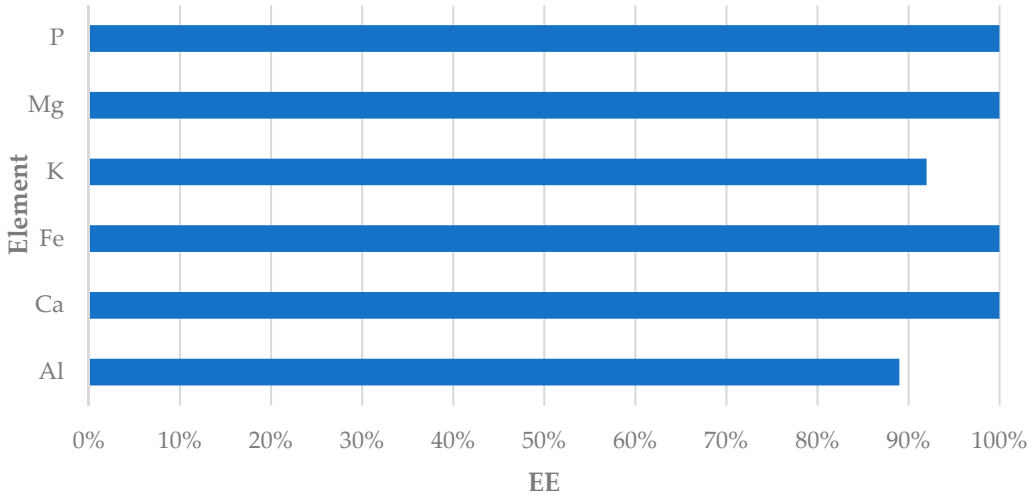

Figure 6. Extraction efficiency (EE) of BC_P (char from a slow pyrolysis test at pilot scale) inorganic elements.

3.5.2. Biocoal (LBC_P) Characterization

The characterization of the biocoal (LBC_P) focused on the total remaining ash content, the resulting concentration of C, H, and N, and the surface area (Table 10).

In total, due to ash extraction, the content of carbon and nitrogen in the biocoal increased by 67% and 77%, respectively. The porosity increased as well, from 7 to 17 $m^2\ g^{-1}$. LBC_P mass yield by the leaching process, calculated according to Equation (3), resulted in 48.2% d.b. The elemental analysis of LBC_p is reported in Table 11.

Table 10. Proximate and ultimate analysis, and surface area of the biocoal (LBC_P).

Parameter	LBC_P	Unit
Ash (710 °C)	9.2	% d.b.
Volatiles	31.4	% d.b.
Carbon (C)	59.4	% d.b.
Hydrogen (H)	3.1	% d.b.
Nitrogen (N)	11.0	% d.b.
Surface area	17.2	m^2g^{-1} d.b.

d.b.—dry basis.

Table 11. Inorganic elements concentration in LBC_P.

Element	Value	Unit
Al	2568	mg/kg d.b.
Ca	b.d.l.	mg/kg d.b.
Cr	b.d.l.	mg/kg d.b.
Fe	9075	mg/kg d.b.
K	1057	mg/kg d.b.
Mg	528	mg/kg d.b.
Mn	b.d.l.	mg/kg d.b.
Na	334	mg/kg d.b.
Ni	43	mg/kg d.b.
P	b.d.l.	mg/kg d.b.
Pb	b.d.l.	mg/kg d.b.
Ti	186	mg/kg d.b.
Zn	40	mg/kg d.b.

3.6. Inorganics Recovery by Precipitation

The inorganic compounds extracted by chemical leaching were recovered by precipitation. The composition of the acid liquid (LL_P) resulting from LBC_P leaching is reported in Table 12.

Table 12. Inorganic elements concentrations in leachate (LL_P).

Element	LL	Unit
Al	459	mg/kg
Ca	4388	mg/kg
Cr	1.7	mg/kg
Fe	5082	mg/kg
K	218	mg/kg
Mg	316	mg/kg
Mn	57	mg/kg
Na	230	mg/kg
P	3233	mg/kg
Si	57	mg/kg
Zn	43	mg/kg

The mass balance of the precipitation process is reported in Table 13.

Table 13. Mass balance of the precipitation test.

Material	Mass (g)
Leachate (LL)	100
Dosed alkaline solution	28.6
Of which:	
• Water	24.3
• Pure KOH	4.3

Table 13. *Cont.*

Material	Mass (g)
Precipitation liquid (PL)	123.5
Dry precipitated salt (PS)	5.1
Precipitated salt moisture	28.3

As the table shows, a precipitated salt (PS) mass yield of approximately 5.1% was obtained from the LL_P. Both the PS and the precipitation liquid (PL) obtained by the process were characterized to determine the performance of the process. The composition of both fractions is reported in Table 14.

Table 14. Inorganic elements concentration in the PS (precipitated salt) and in the PL (precipitation liquid) recovered after precipitation.

Element	PS	PL	Unit
Al	9434	0	mg/kg d.b.
Ca	50,200	2942	mg/kg d.b.
Cr	27	0	mg/kg d.b.
Fe	109,459	14	mg/kg d.b.
K	192,260	10,609	mg/kg d.b.
Mg	5819	49	mg/kg d.b.
Mn	1243	0	mg/kg d.b.
Na	2742	302	mg/kg d.b.
P	69,965	0	mg/kg d.b.
Pb	29	1	mg/kg d.b.
Zn	805	0	mg/kg d.b.

d.b.—dry basis.

The recovery efficiency of the precipitation process was calculated considering the remaining fraction of each single element in the PL. The analysis shows that the PL contained only 2942 mg kg^{-1} of Ca, 10,609 mg kg^{-1} of K, 14 mg kg^{-1} of Fe, and 302 mg g^{-1} of Na. High recovery of all elements was achieved, with a 100% recovery for both P and Al. The PL could be reused in the precipitation process for the KOH solution preparation.

3.7. Activated Carbon Production

The activation process, performed at 700 °C and 800 °C in a tubular furnace, produced two activated carbons (AC1 and AC2) with a mass yield of 75.5% and 66.8%, respectively. The composition of the two products is reported in Table 15.

Table 15. Activated carbon analysis and mass yield (AC1: activated carbon produced at 700 °C, AC2: activated carbon produced at 800 °C).

Processed Biocoal	AC1	AC2	Unit
Mass yield	75.5	66.8	% d.b.
Ash (710 °C)	14.0	15.3	% d.b.
Carbon (C)	72.3	73.0	% d.b.
Hydrogen (H)	1.1	0.8	% d.b.
Nitrogen (N)	9.0	6.8	% d.b.
BET Surface area	353	417	m^2 g^{-1} d.b.

d.b.—dry basis.

AC1 showed a higher mass yield, but also a lower porosity and a higher nitrogen content. AC2, produced at 800 °C, resulted in a higher surface area and a lower nitrogen content. The lower concentration of nitrogen in AC2 can be attributed to the higher activation temperature, which led to the devolatilization of the nitrogen compounds. However, the mass yield obtained at 800 °C is about 11.7% less than at 700 °C.

In addition to the BET surface area (reported in Table 15), the DFT surface area and average pore volume were analyzed, and their trend is shown by Figures 7 and 8. AC1 resulted in 0.192 cm^3 g^{-1} as the total pore volume for a DFT surface area of 325 m^2 g^{-1}. AC2 resulted in 0.239 cm^3 g^{-1} as the total pore volume for a DFT surface area of 510 m^2 g^{-1}.

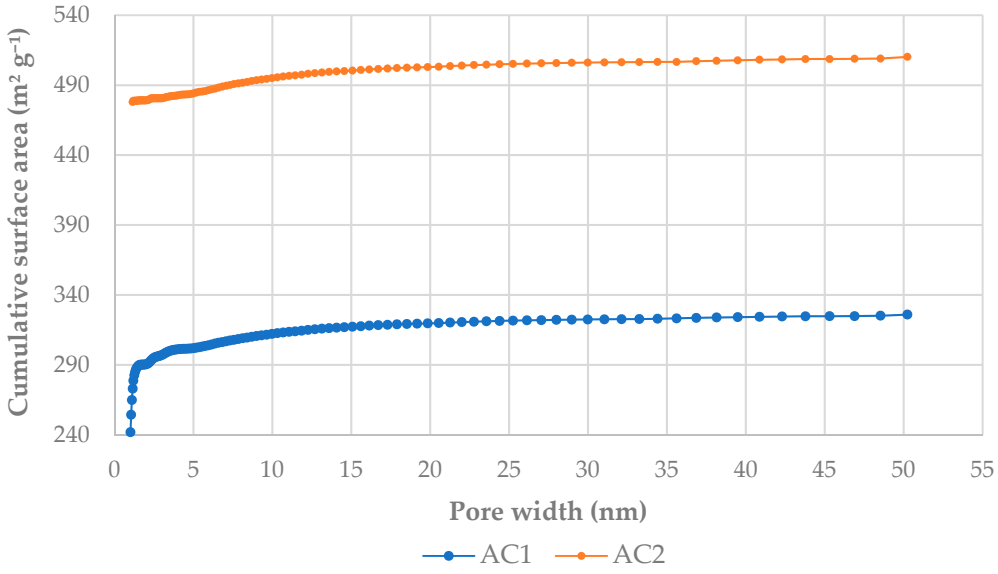

Figure 7. Trend of the cumulative surface area compared to AC1 (activated carbon produced at 700 °C) and AC2 (activated carbon produced at 800 °C) pore width.

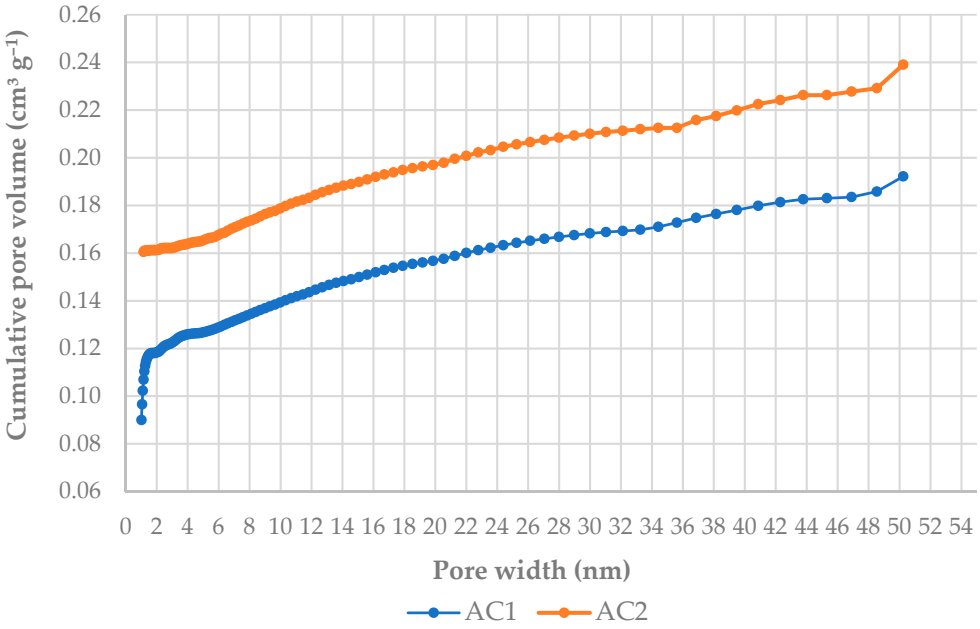

Figure 8. Trend of the cumulative pore volume compared to AC1 (activated carbon produced at 700 °C) and AC2 (activated carbon produced at 800 °C) pore width.

Figure 8 reports AC1 and AC2 cumulative pore volume (y axis) compared to pore width (x axis). The graph shows that the total pore volume in AC1 was mainly generated by micropores (pore size < 2 nm), with an average pore width of 1.1 nm, contributing to about 61.6% of the total pore volume. Similarly, AC2 showed an average pore width of 1.4 nm, contributing about 67.5% of the total pore volume. From the mentioned analysis, the two activated carbons result in prevalently microporous materials.

The alpha-S method was adopted to confirm the DFT method results for AC1 and AC2. In general, the alpha-S plot consists of the trend of the adsorbed N_2 volume (in standard temperature and pressure conditions) against alpha-s (the ratio between the amount adsorbed by a reference non-porous sample and the amount adsorbed at a relative pressure of 0.4) [40]. For AC1, the alpha-S plot had a slope of 23.9 and an intercept of 74.0 cm^3 g^{-1}; for AC2, the alpha-S plot had a slope of 23.7 and an intercept of 101.8 cm^3 g^{-1}. From this method, the micro-pore volume (<2 nm) of AC1 resulted in 0.114 cm^3 g^{-1}, which is consistent with that produced by DFT (Figure 8), equal to 0.118 cm^3 g^{-1}. The volume of AC2 micropores by alpha-S plot (0.157 cm^3 g^{-1}) is consistent with that from DFT (0.162 cm^3 g^{-1}) as well.

The total mass yield (ACY) achieved considering the three process steps (pyrolysis, leaching, and activation) resulted in 15.6% d.b. for AC1 and 13.8% d.b. for AC2. The porosity achieved at 800 °C resulted in up to double that obtained by physical or chemical activation of sewage sludge char in other studies [41,42].

The FT-IR spectra of AC1 and AC2 are reported in Figure 9, compared to those of a commercial activated carbon.

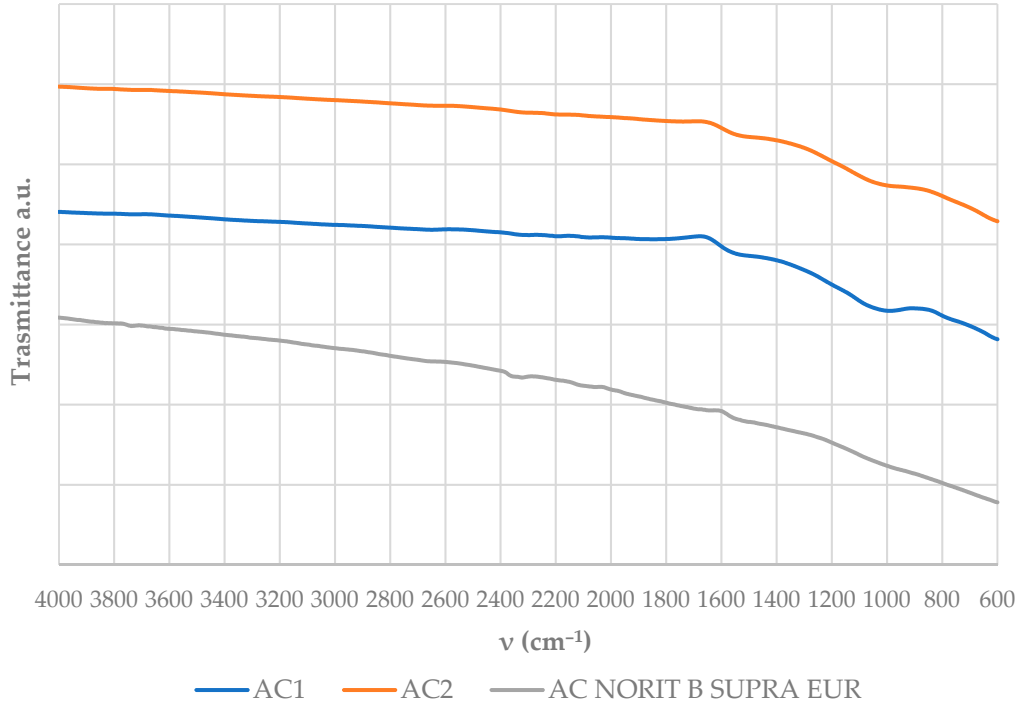

Figure 9. FT-IR analysis of the obtained activated carbons AC1 (activated carbon produced at 700 °C) and AC2 (activated carbon produced at 800 °C) in comparison with a commercial product (AC NORIT B SUPRA EUR). Notation: a.u.—arbitrary unit, ν—wavenumber.

4. Discussion

Carbon, hydrogen, and nitrogen decreased with the increase in slow pyrolysis temperature (Table 5), as temperature affects the devolatilization of organic compounds. About 6.1% nitrogen was found in the solid produced at 400 °C, while less than 4% was found in that produced at 650 °C (Table 5). Nitrogen is estimated to be present in the sludge, mainly in the form of protein N (P-N). In fact, according to [43], despite the fact that pyridine N (N-6), pyrrole N (N-5), and nitrogen oxides have been found in the sludge, P-N and N-6 often represent more than 80% of the total N. On the contrary, sulfur increases (Table 5), probably due to the high stability of sulfur compounds and the presence of inorganic sulfur [44].

As shown in Figure 3, the DD achieved by the chemical leaching tests on the char produced on a laboratory scale slightly increases for the char produced at 450 °C in com-

parison with that obtained at 400 °C. This can be due to the solubility of the char organic matter produced at 400 °C, which reacts under leaching conditions, reducing the efficacy of leaching on inorganic compounds. At temperatures higher than 450 °C, the DD gradually decreases with increasing pyrolysis temperatures. This result is probably due to the reduction of the solubility of P, Ca, and other heavy metal compounds with the increase in temperature. The reduction of both heavy metals and P-Ca compounds solubility at higher pyrolysis temperatures has been widely investigated in several studies. A higher Ca-P crystallinity was found in the chars produced at high pyrolysis temperatures, correlated with low water-extractable P [45], and a reduced availability of phosphorus was identified above 600 °C pyrolysis [46]. A reduced solubility was also found for other heavy metals when the pyrolysis temperature increased from 500 to 800 °C [47]. The pyrolysis trials performed in the pilot plant showed a lower char mass yield compared to that obtained in the laboratory at the same temperature. However, the composition of the char obtained at the pilot scale was similar to that produced in the laboratory. Therefore, the different mass balance is probably related to the losses or partial combustion of char powder, which could take place during the test in the pilot plant.

Despite the mass yield of the activated carbon compared to the initial processed feedstock resulted from 13.8 to 15.6%, the amount of stored carbon in the produced activated carbons was 28.0% for AC2 and 31.4% for AC1. Thus, it can be estimated that about two-thirds of the carbon retained in the feedstock was devolatilized during the process. Both the obtained activated carbons showed a high surface area, more than 20 times higher than that of the LBC_P. Moreover, carbon concentration increased from 59.4% in LBC_P to 72–73%, while hydrogen was reduced to less than 1 %. These results enabled us to consider both AC1 and AC2 as anthracitic carbons, according to the Van Krevelen coal classification (Figure 10), and hence comparable to those used in the steelmaking sector.

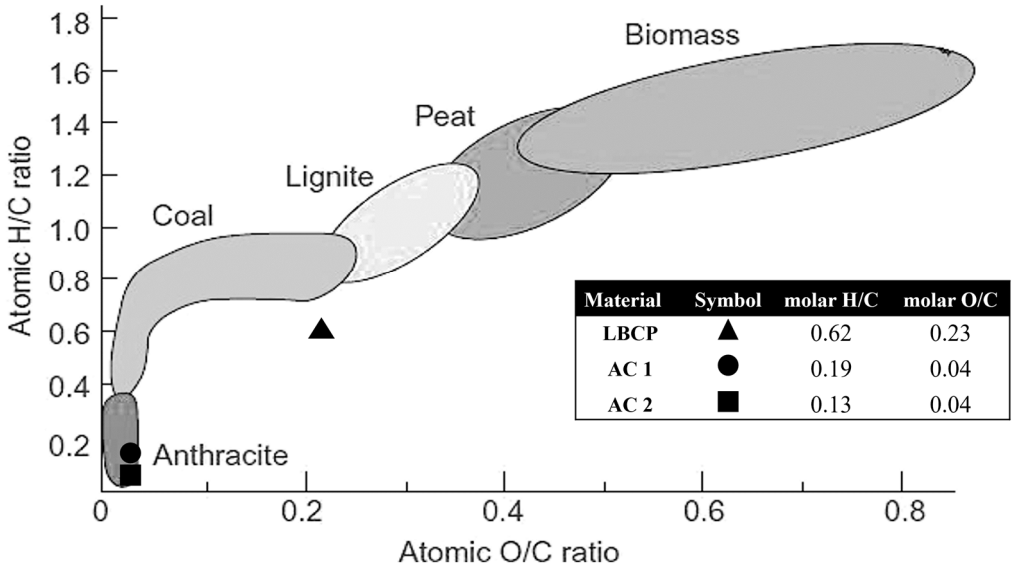

Figure 10. Classification of produced coals by Van Krevelen Diagram [48] (LBC_P: biocoal from leaching test on char from slow pyrolysis test at pilot scale, AC1: activated carbon produced at 700 °C, AC2: activated carbon produced at 800 °C).

Typical properties of the activated carbons are high carbon content, high specific surface areas, and a high level of porosity. The distribution of pores, in combination with the specific surface area, is dependent on the starting materials of activation and on the adopted process parameters [49]. Therefore, specific absorption trials should be performed to better determine the quality of the produced activated carbons. However, the specific surface areas obtained by the tests were comparable to physically activated biomass [49,50].

Since activated carbon has a large specific surface area and has developed micropores, it has strong absorptivity and a large adsorption capacity. Since the physical adsorption properties of activated carbons are mainly related to the specific surface area, it is expected that both AC1 and AC2 could be used as adsorbents in wastewater treatment or in industrial emissions processes. Activated carbon can be used either alone or in combination with other water treatment technologies [51].

The FT-IR spectra of both samples (Figure 9) show a lack of functionalization typical of graphitic material [52]. The spectra appear to be smooth in the region 4000–1700 cm^{-1}, while low signals are detected around 1600 cm^{-1}, from aromatic C=C stretching, and around 1100 cm^{-1}, probably related to inorganic oxides left from the feedstock. The spectra were also compared to a commercial steam-activated charcoal, NORIT B SUPRA EUR, which shows a similar smooth spectrum as the thermally activated samples, with even fewer functional groups detected. The FT-IR analysis enabled us to determine the high graphitization rate of the activated carbons (AC1 and AC2) and their similarity with commercial adsorbents available on the market [53]. The precipitated salt showed a high concentration of P, Ca, and Fe, including a relevant content of K derived from the KOH dosed for the precipitation test. In particular, converting the P and K concentrations resulting from PS analysis into equivalent P_2O_5 and K_2O, the resulting concentrations are 16% P_2O_5 and 23% K_2O. The composition of the obtained precipitated salt was compared to that reported in the current Italian regulation on fertilizers [54] (and following modifications). The obtained precipitate could be potentially framed as a couple of fertilizing products included by the decree, that is, mixed phosphate salts that shall have a minimum 10% P_2O_5 concentration, or PK fertilizers, named "concimi PK", whose requirements include minimum P_2O_5 and K_2O concentrations of 5% each and a minimum overall concentration (P_2O_5 + K_2O) of 18% [55]. The concentration of P, as P_2O_5, and K, as K_2O, resulted largely above the minimum values required by the decree.

Moreover, the concentration of P_2O_5 was in line with that required by the EU FPR for precipitated phosphate salts (recognized as Component Material Category 12). The high concentration of iron, above the 10% d.b. EU FPR limit for precipitated phosphate salts, could represent a limit for the marketability of the product in the fertilizer industry, despite the fact that iron is not considered a toxic element. However, due to the low precipitation pH of iron ions, a two-stage selective precipitation could be performed to separately collect iron and increase the quality of the inorganic fertilizer.

5. Conclusions

The study demonstrated that the sludge produced by industrial WWTPs could be a valuable source of carbon and inorganic nutrients to be recycled as end-of-waste products with high added value. The industrial sludge processed in this study showed a similar composition to civil sludge but with a much lower silica content. The lack of silicates in the sludge and, thus, in the char enabled a high degree of demineralization by a single-step acid leaching. The biocoal obtained after low-temperature slow pyrolysis and chemical leaching presented a high nitrogen and volatile content and a low surface area (17.2 m^2 g^{-1}), which reduced its quality as a substitute for fossil coal. On the contrary, activation enabled a strong reduction of nitrogen, and increased carbon content to up to 73.2% d.b., and produced a material with a high surface area (470 m^2 g^{-1}) that was potentially usable as an adsorbent for liquid or gas effluents. The recovery of the inorganics from the leachate by precipitation in a single step led to the formation of a precipitated salt with a high concentration of P and K but also containing the full amount of iron contained in the initial sludge. The separated collection and, thus, the reduction of iron concentration in the salt could lead to an increase in the value of the obtained product.

Author Contributions: All authors contributed to the study's conception and design. Material preparation, test conduction, data collection, and analysis were performed by A.S. and M.D.B. The first draft of the manuscript was written by A.S. and edited and commented on by A.M.R. and all other authors. All authors have read and agreed to the published version of the manuscript.

Funding: This research was funded by the project H2STEEL "Green H2 and circular bio-coal from biowaste for cost-competitive sustainable Steel", funded by the European Commission HORIZON-EIC-2021-PATHFINDERCHALLENGES-01-04-Novel routes to green hydrogen production, grant number 101070741.

Data Availability Statement: Data is contained within this article. Additional data is available from the corresponding author on reasonable request.

Acknowledgments: The authors acknowledge the project H2STEEL "Green H2 and circular bio-coal from biowaste for cost-competitive sustainable Steel", funded by the European Commission HORIZON-EIC-2021-PATHFINDERCHALLENGES-01-04-Novel routes to green hydrogen production. Moreover, authors acknowledge Lorenzo Bettucci, Mattia Monastra, Samuele Zanieri, and Giulia Lotti for their efforts in providing an accurate characterization of the produced materials.

Conflicts of Interest: The authors declare that they have no known competing financial interest or personal relationships that could have appeared to influence the work reported in this paper.

Nomenclature

WWTP	Wastewater treatment plant
EEA	European Environment Agency
EU FPR	European Union Fertilizing Products Regulation
EU ETS	European Union Emission Trading Scheme
HTC	Hydrothermal Carbonization
PT_{400}	laboratory scale slow pyrolysis test performed at 400 °C
PT_{450}	laboratory scale slow pyrolysis test performed at 450 °C
PT_{500}	laboratory scale slow pyrolysis test performed at 500 °C
PT_{550}	laboratory scale slow pyrolysis test performed at 550 °C
PT_{600}	laboratory scale slow pyrolysis test performed at 600 °C
PT_{650}	laboratory scale slow pyrolysis test performed at 650 °C
PT_P	pilot scale slow pyrolysis test
Char	solid obtained after slow pyrolysis
BC	char from slow pyrolysis test at lab scale
BC_P	char from slow pyrolysis test at pilot scale
AP	Aqueous Phase
LOP	Light Oil Phase
HOP	Heavy Oil Phase
LT_{400}	leaching test performed on the char produced by PT_{400}
LT_{450}	leaching test performed on the char produced by PT_{450}
LT_{500}	leaching test performed on the char produced by PT_{500}
LT_{550}	leaching test performed on the char produced by PT_{550}
LT_{600}	leaching test performed on the char produced by PT_{600}
LT_{650}	leaching test performed on the char produced by PT_{650}
LT_P	leaching test performed on the char produced by PT_P
Biocoal	solid from char leaching test
LBC	biocoal from leaching test on BC
LBC_P	biocoal from leaching test on BC_P
LL_P	leachate from LT_P
DD	Degree of Demineralization
EE	Extraction Efficiency
PL	Precipitation Liquid
PS	dry precipitated salt
AT1	activation test performed at 700 °C
AT2	activation test performed at 800 °C
AC1	activated char from AT1
AC2	activated char from AT2
PMY	mass yield of char from PT_P
LMY	mass yield of char from LT_P
AMY	mass yield of char activation tests
ACY_{tot}	mass yield of activated chars, including PMY, LMY and AMY

References

1. Granger, M.; Montalvo, D. *Industrial Waste Water Treatment—Pressure on Europe's Environment*; Publications Office of the European Union: Luxembourg, 2019.
2. Food and Agriculture Organization of the United Nations. AQUASTAT Main Database. Available online: https://tableau.apps.fao.org/views/ReviewDashboard-v1/country_dashboard?%3Adisplay_count=n&%3Aembed=y&%3AisGuestRedirectFromVizportal=y&%3Aorigin=viz_share_link&%3AshowAppBanner=false&%3AshowVizHome=n (accessed on 1 June 2023).
3. European Commission. *Evaluation of the Council Directive 91/271/EEC of 21 May 1991, Concerning Urban Waste-Water Treatmen*; European Commission: Bruxelles, Belgium, 2019.
4. Büttner, O.; Jawitz, J.W.; Birk, S.; Borchardt, D. Why wastewater treatment fails to protect stream ecosystems in Europe. *Water Res.* **2022**, *217*, 118382. [CrossRef] [PubMed]
5. EurEau. Position paper on Industrial Waste Water Discharges into Sewers. 2021. Available online: https://www.eureau.org/resources/position-papers/6074-eureau-position-paper-on-industrial-waste-water-discharges-into-sewers/file (accessed on 6 May 2023).
6. Anderson, N.; Snaith, R.; Madzharova, G.; Bonfait, J.; Doyle, L.; Godley, A.; Lam, M.; Day, G. *Sewage Sludge and the Circular Economy From: Ricardo Energy and Environment*; European Environment Agency (EEA): Strasbourg, France, 2021.
7. *Beyond Water Quality-Sewage Treatment in a Circular Economy*; Publications Office of the European Union: Luxembourg, 2022. [CrossRef]
8. Ragazzi, M.; Rada, E.C.; Ferrentino, R. Analysis of real-scale experiences of novel sewage sludge treatments in an Italian pilot region. *Desalination Water Treat.* **2014**, *55*, 783–790. [CrossRef]
9. Kacprzak, M.; Neczaj, E.; Fijałkowski, K.; Grobelak, A.; Grosser, A.; Worwag, M.; Rorat, A.; Brattebo, H.; Almås, Å.; Singh, B.R. Sewage sludge disposal strategies for sustainable development. *Environ. Res.* **2017**, *156*, 39–46. [CrossRef] [PubMed]
10. Samolada, M.C.; Zabaniotou, A.A. Comparative assessment of municipal sewage sludge incineration, gasification and pyrolysis for a sustainable sludge-to-energy management in Greece. *Waste Manag.* **2014**, *34*, 411–420. [CrossRef]
11. Fytili, D.; Zabaniotou, A. Utilization of sewage sludge in EU application of old and new methods—A review. *Renew. Sustain. Energy Rev.* **2008**, *12*, 116–140. [CrossRef]
12. Siebielska, I. Comparison of changes in selected polycyclic aromatic hydrocarbons concentrations during the composting and anaerobic digestion processes of municipal waste and sewage sludge mixtures. *Water Sci. Technol.* **2014**, *70*, 1617–1624. [CrossRef] [PubMed]
13. Ferrentino, R.; Langone, M.; Fiori, L.; Andreottola, G. Full-Scale Sewage Sludge Reduction Technologies: A Review with a Focus on Energy Consumption. *Water* **2023**, *15*, 615. [CrossRef]
14. Mew, M.C.; Steiner, G.; Geissler, B. Phosphorus Supply Chain—Scientific, Technical, and Economic Foundations: A Transdisciplinary Orientation. *Sustainability* **2018**, *10*, 1087. [CrossRef]
15. Law, K.P.; Pagilla, K.R. Reclaimed phosphorus commodity reserve from water resource recovery facilities—A strategic regional concept towards phosphorus recovery. *Resour. Conserv. Recycl.* **2019**, *150*, 104429. [CrossRef]
16. Magrí, A.; Carreras-Sempere, M.; Biel, C.; Colprim, J. Recovery of Phosphorus from Waste Water Profiting from Biological Nitrogen Treatment: Upstream, Concomitant or Downstream Precipitation Alternatives. *Agronomy* **2020**, *10*, 1039. [CrossRef]
17. European Parliament. *EU Fertilising Products Regulation*; European Parliament: Bruxelles, Belgium, 2019.
18. Adionics. *Critical Raw Materials: Ensuring Secure and Sustainable Supply Chains for EU's Green and Digital Future*; Adionics: Les Ulis, France, 2023.
19. Critical Raw Materials Resilience: Charting a Path towards greater Security and Sustainability 1. 2020. Available online: http://info.worldbank.org/governance/wgi/ (accessed on 6 May 2023).
20. Directive 2003/87/EC of the European Parliament and of the Council of 13 October 2003 Establishing a Scheme for Greenhouse Gas Emission Allowance Trading within the Community and Amending Council Directive 96/61/EC (Text with EEA Relevance). 2003. Available online: https://eur-lex.europa.eu/legal-content/EN/TXT/?uri=celex%3A32003L0087 (accessed on 6 May 2023).
21. EU Carbon Permits. Available online: https://tradingeconomics.com/commodity/carbon (accessed on 1 June 2023).
22. Zhang, X.; Du, D.; Wu, Y.; Ye, P.; Xu, Y. Theoretical and analytical solution on vacuum preloading consolidation of landfill sludge treated by freeze–thaw and chemical preconditioning. *Acta Geotech.* **2023**, 1–18. [CrossRef]
23. Zhang, X.; Ye, P.; Wu, Y. Enhanced technology for sewage sludge advanced dewatering from an engineering practice perspective: A review. *J. Environ. Manag.* **2022**, *321*, 115938. [CrossRef] [PubMed]
24. Gao, N.; Kamran, K.; Quan, C.; Williams, P.T. Thermochemical conversion of sewage sludge: A critical review. *Prog. Energy Combust. Sci.* **2020**, *79*, 100843. [CrossRef]
25. Barry, D.; Barbiero, C.; Briens, C.; Berruti, F. Pyrolysis as an economical and ecological treatment option for municipal sewage sludge. *Biomass Bioenergy* **2019**, *122*, 472–480. [CrossRef]
26. Tasca, A.L.; Puccini, M.; Gori, R.; Corsi, I.; Galletti, A.M.R.; Vitolo, S. Hydrothermal carbonization of sewage sludge: A critical analysis of process severity, hydrochar properties and environmental implications. *Waste Manag.* **2019**, *93*, 1–13. [CrossRef] [PubMed]

27. Aragón-Briceño, C.I.; Ross, A.B.; Camargo-Valero, M.A. Mass and energy integration study of hydrothermal carbonization with anaerobic digestion of sewage sludge. *Renew. Energy* **2021**, *167*, 473–483. [CrossRef]
28. Malhotra, M.; Garg, A. Hydrothermal Carbonization of Sewage Sludge: Optimization of Operating Conditions Using Design of Experiment Approach and Evaluation of Resource Recovery Potential. *J. Environ. Chem. Eng.* **2023**, *11*, 109507. [CrossRef]
29. Staf, M.; Buryan, P. Slow pyrolysis of pre-dried sewage sludge. *Chem. Pap.* **2016**, *70*, 1479–1492. [CrossRef]
30. Mphahlele, K.; Matjie, R.H.; Osifo, P.O. Thermodynamics, kinetics and thermal decomposition characteristics of sewage sludge during slow pyrolysis. *J. Environ. Manag.* **2021**, *284*, 112006. [CrossRef] [PubMed]
31. Lee, Y.; Park, J.; Ryu, C.; Gang, K.S.; Yang, W.; Park, Y.-K.; Jung, J.; Hyun, S. Comparison of biochar properties from biomass residues produced by slow pyrolysis at 500 °C. *Bioresour. Technol.* **2013**, *148*, 196–201. [CrossRef]
32. Salimbeni, A.; Di Bianca, M.; Lombardi, G.; Rizzo, A.M.; Chiaramonti, D. Opportunities of Integrating Slow Pyrolysis and Chemical Leaching for Extraction of Critical Raw Materials from Sewage Sludge. *Water* **2023**, *15*, 1060. [CrossRef]
33. Xu, L.; Chen, Y.; Liu, M.; Fu, X. Comparison of Phosphorus Extraction from Sludge Incinerated Bottom Ash and Sludge Incinerated Fly Ash Using Sulfuric Acid. *Environ. Eng. Sci.* **2020**, *37*, 637–645. [CrossRef]
34. Shiba, N.C.; Ntuli, F. Extraction and precipitation of phosphorus from sewage sludge. *Waste Manag.* **2017**, *60*, 191–200. [CrossRef]
35. Liu, H.; Hu, G.; Basar, I.A.; Li, J.; Lyczko, N.; Nzihou, A.; Eskicioglu, C. Phosphorus recovery from municipal sludge-derived ash and hydrochar through wet-chemical technology: A review towards sustainable waste management. *Chem. Eng. J.* **2021**, *417*, 129300. [CrossRef]
36. Ghorbani, M.; Konvalina, P.; Walkiewicz, A.; Neugschwandtner, R.W.; Kopecký, M.; Zamanian, K.; Chen, W.-H.; Bucur, D. Feasibility of Biochar Derived from Sewage Sludge to Promote Sustainable Agriculture and Mitigate GHG Emissions—A Review. *Int. J. Environ. Res. Public Health* **2022**, *19*, 12983. [CrossRef] [PubMed]
37. Gopinath, A.; Divyapriya, G.; Srivastava, V.; Laiju, A.; Nidheesh, P.; Kumar, M.S. Conversion of sewage sludge into biochar: A potential resource in water and wastewater treatment. *Environ. Res.* **2021**, *194*, 110656. [CrossRef] [PubMed]
38. Oliver-Tomas, B.; Hitzl, M.; Owsianiak, M.; Renz, M. Evaluation of hydrothermal carbonization in urban mining for the recovery of phosphorus from the organic fraction of municipal solid waste. *Resour. Conserv. Recycl.* **2019**, *147*, 111–118. [CrossRef]
39. Pérez, C.; Boily, J.-F.; Jansson, S.; Gustafsson, T.; Fick, J. Acid-Induced Phosphorus Release from Hydrothermally Carbonized Sewage Sludge. *Waste Biomass Valorization* **2021**, *12*, 6555–6568. [CrossRef]
40. Sing, K.S.W.; Williams, R.T. Review Empirical Procedures for the Analysis of Physisorption Isotherms. *Adsorpt. Sci. Technol.* **2005**, *23*, 839–853. [CrossRef]
41. Lu, G.; Lau, D. Characterisation of sewage sludge-derived adsorbents for H2S removal. Part 2: Surface and pore structural evolution in chemical activation. *Gas Sep. Purif.* **1996**, *10*, 103–111. [CrossRef]
42. Almahbashi, N.; Kutty, S.; Ayoub, M.; Noor, A.; Salihi, I.; Al-Nini, A.; Jagaba, A.; Aldhawi, B.; Ghaleb, A. Optimization of Preparation Conditions of Sewage sludge based Activated Carbon. *Ain Shams Eng. J.* **2020**, *12*, 1175–1182. [CrossRef]
43. Wei, L.; Wen, L.; Yang, T.; Zhang, N. Nitrogen Transformation during Sewage Sludge Pyrolysis. *Energy Fuels* **2015**, *29*, 5088–5094. [CrossRef]
44. Huang, R.; Tang, Y.; Luo, L. Thermochemistry of sulfur during pyrolysis and hydrothermal carbonization of sewage sludges. *Waste Manag.* **2020**, *121*, 276–285. [CrossRef]
45. Zwetsloot, M.J.; Lehmann, J.; Solomon, D. Recycling slaughterhouse waste into fertilizer: How do pyrolysis temperature and biomass additions affect phosphorus availability and chemistry? *J. Sci. Food Agric.* **2014**, *95*, 281–288. [CrossRef]
46. Bruun, S.; Harmer, S.L.; Bekiaris, G.; Christel, W.; Zuin, L.; Hu, Y.; Jensen, L.S.; Lombi, E. The effect of different pyrolysis temperatures on the speciation and availability in soil of P in biochar produced from the solid fraction of manure. *Chemosphere* **2017**, *169*, 377–386. [CrossRef] [PubMed]
47. Larina, O.M.; Zaichenko, V.M. Influence of pyrolysis on evaporation and solubility of heavy metals in sewage sludge. *J. Phys. Conf. Ser.* **2020**, *1556*, 012017. [CrossRef]
48. van Krevelen, D.W. *Coal—Typology, Physics, Chemistry, Constitution*, 3rd ed.; Elsevier: Amstedam, The Netherlands; New York, NY, USA, 1993. Available online: https://openlibrary.org/books/OL1147163M/Coal{-}{-}typology_physics_chemistry_constitution (accessed on 25 April 2023).
49. Bergna, D.; Varila, T.; Romar, H.; Lassi, U. Comparison of the Properties of Activated Carbons Produced in One-Stage and Two-Stage Processes. *C* **2018**, *4*, 41. [CrossRef]
50. Ngernyen, Y.; Tangsathitkulchai, C.; Tangsathitkulchai, M. Porous properties of activated carbon produced from Eucalyptus and Wattle wood by carbon dioxide activation. *Korean J. Chem. Eng.* **2006**, *23*, 1046–1054. [CrossRef]
51. Jiang, C.; Cui, S.; Han, Q.; Li, P.; Zhang, Q.; Song, J.; Li, M. Study on Application of Activated Carbon in Water Treatment. *IOP Conf. Ser. Earth Environ. Sci.* **2019**, *237*, 022049. [CrossRef]
52. Chen, X.; Lai, X.; Hu, J.; Wan, L. An easy and novel approach to prepare Fe_3O_4–reduced graphene oxide composite and its application for high-performance lithium-ion batteries. *RSC Adv.* **2015**, *5*, 62913–62920. [CrossRef]
53. Tsang, D.C.W.; Hu, J.; Liu, M.Y.; Zhang, W.; Lai, K.C.K.; Lo, I.M.C. Activated Carbon Produced from Waste Wood Pallets: Adsorption of Three Classes of Dyes. *Water Air Soil Pollut.* **2007**, *184*, 141–155. [CrossRef]

54. Gazzetta Ufficiale Della Repubblica Italiana. Decreto Legislativo 29 Aprile 2010, n. 75—Riordino e Revisione Della Disciplina in Materia di Fertilizzanti, a Norma Dell'articolo 13 Della Legge 7 Luglio 2009, n. 88. 2010. Available online: https://www.politicheagricole.it/flex/cm/pages/ServeBLOB.php/L/IT/IDPagina/10087 (accessed on 10 June 2023).
55. Gazzetta Ufficiale Della Repubblica Italiana. Decreto Legislativo 10 Ottobre 2022—Aggiornamento Degli Allegati 1, 6, 7, 8, 9, 13 e 14 al Decreto Legislativo n. 75 del 29 Aprile 2010, Recante: «Riordino e Revisione Della Disciplina in Materia di Fertilizzanti, a Norma Dell'articolo 13 Della Legge 7 Luglio 2009, n. 88». 2022. Available online: https://www.gazzettaufficiale.it/eli/id/2022/12/29/22A07263/sg (accessed on 10 June 2023).